

System Design of Electric Assisted Bicycle using EDLCs and Wireless Charger

Jun-ichi Itoh, Kenji Noguchi and Koji Orikawa

Department of Electrical, Electronics and Information Engineering
Nagaoka University of Technology
Nagaoka, Niigata, Japan

itoh@vos.nagaokaut.ac.jp, k_noguchi@stn.nagaokaut.ac.jp, orikawa@vos.nagaokaut.ac.jp

Abstract— This paper discusses an electric assisted bicycle which uses electric double layer capacitors (EDLCs) as a power source. EDLCs are charged through a rapid charger by using wireless power transmission. In this paper, first, the energy capacity of EDLCs is designed. Next, the antenna for the wireless power transmission and the charger are investigated. Third, this paper compares the volume and the power loss of the three kinds of DC-DC converters which are step-down type, boost-type and buck-boost type for the charging and discharging of EDLCs. As a result, boost-type is the most compact in the power capacity of the electric assisted bicycle. Finally, the proposed system is experimentally verified as a prototype. As a result, the proposed system can shorten to 1/4 the charging time of the conventional system.

Keywords— *Electric assisted bicycle, Electric double layer capacitors, Wireless power transfer, System design*

I. INTRODUCTION

Recently, electric assisted bicycles have been attracted because the safety and easy driving on bicycle. The electric assisted bicycles use a lithium-ion battery as energy source. The lithium-ion battery is suitable for a long assist time owing to high energy density. However the lithium-ion battery is the short lifetime and the necessary to the long charging time.

On the other hands, the electric vehicle using electric double layer capacitors (EDLCs) of long cycle life has been developed as city commuters [1]. This system uses EDLCs instead of the lithium-ion battery. However, the large vehicle such as a car is afraid of the empty of the energy on the load.

The electric bike with EDLCs has been also proposed [2]. The EDLCs are suitable for the electric bike owing to the small vehicle. However, the electric bike is also afraid of the empty of the energy.

This paper proposes an electric assisted bicycle with EDLCs [3]. The electric assisted bicycle is not afraid of the empty of the energy because it can be driven by pedals on the bicycle even if no electric energy. The concept of this system has two concepts as follows; First, it is assumed that the EDLCs are used as only the assist of starting acceleration and slopes for the electric assisted bicycle in order to suppress the total energy of the EDLCs; Second, the wireless power transfer system is

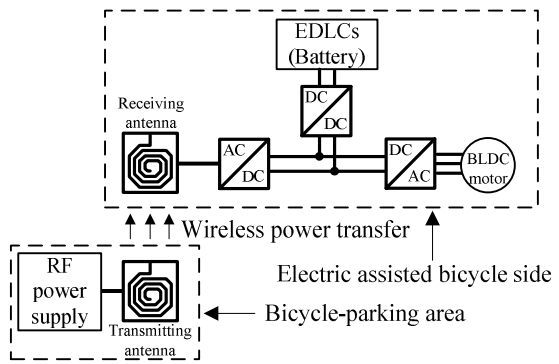


Fig. 1. Configuration of the proposed system. The proposed system can be charged by simply park the electric assisted bicycle to bicycle parking area.

applied to rapid charger for the EDLCs because of small capacity and the short charging time.

In order to maximize the advantages of the proposed system, it is necessary to optimize the design from the perspective of the overall system in consideration of trade-off problem of the time required to fully charge the EDLCs and the total volume of the power conversion system.

Therefore, as the purpose of optimum design of the proposed system, this paper evaluates three items as follows;

- 1) The energy capacity of EDLCs which is required for assist, based on the running test,
- 2) The antenna using a print circuit board (PCB) and charger design for the wireless power transmission,
- 3) The circuit topology of the interface DC-DC converter for EDLCs in the proposed system configuration in terms of the volume and efficiency.

Finally, the proposed system is experimentally verified as the prototype.

II. PROPOSED SYSTEM CONFIGURATION

Fig. 1 shows the configuration of the proposed system. The proposed system uses a Radio Frequency (RF) power supply at the input stage of the transmitting antenna for wireless power transmission [4-8]. Also, the proposed system comprises a rapid rechargeable AC-DC converter and EDLCs in the latter part of the receiving antenna. In addition, the interface DC-DC converter for the assist

performs discharging control of the EDLCs by assisting the drivers when a brushless DC (BLDC) motor is driven. It is noted that the BLDC motor and DC-AC converter are commercial products [9].

III. DESIGN OF ENERGY CAPACITY OF EDLCs

A. Conditions of Assist

Fig. 2 shows the assist pattern of a driving test. The pattern A is a driving pattern for the evaluation of the assist in the accelerating mode. The pattern B is a driving pattern for demonstration of the assist in the climbing slopes with a gradient (average gradient 6%).

B. Measurement of Cumulative Energy

Fig. 3 shows the method of measuring the cumulative energy of each assist pattern. The energy consumption by pattern A or pattern B is measured using a power meter. The cumulative energy is measured in the conventional system.

Fig. 4 shows the time characteristics of the cumulative energy of each assist pattern. The energy for the assist is 716 J (the energy is 436 J during acceleration time) in the pattern A, and that of the pattern B is 10.6 kJ. From the results in the pattern B, when the distance climbing the distance of the hill was set to 1 km, the necessary energy becomes 53.0 kJ. This paper designs the capacitance of EDLCs that can only assist this energy. Further, the volume of the EDLCs with lithium-ion battery is compared. In addition, the total volume and power loss for three types DC-DC converters using EDLCs as a power source are compared. In addition, the energy of EDLCs is designed in 12.1kJ as a prototype of the system in Section 6.

C. Comparison of Energy

Fig. 5 shows the relationship between the energy and volume of the EDLCs (Nippon Chemi-Con Co, DDLE2R5LGN232KCH2S) and lithium-ion battery in the marketplace [9-10].

The energy E of EDLCs is calculated by (1) where C_{total} is the total capacitance of EDLCs, V_{max} is the maximum voltage of EDLCs (The rated voltage of EDLC per unit is 2.5 V. In this case, the maximum voltage is designed to 22.5 V), V_{min} is the minimum voltage of EDLCs that is designed by the designer (In this case, the minimum voltage is designed to 8 V). The number and the output voltage range of the EDLCs are designed when the charging and discharging energy of EDLCs meet more than 53.0 kJ.

$$E = \frac{1}{2} C_{total} (V_{max}^2 - V_{min}^2) \quad (1)$$

As shown in Fig. 5, the energy E , which is supplied from the EDLCs is designed to 56.5 kJ. Furthermore, the energy density of the EDLCs in the marketplace is 5.16 Wh/dm³. When the energy density becomes more than 1.5 times of the present EDLCs, the energy source size of the proposed system can become smaller than that of the conventional systems. In other words, if the distance of 2/3 is considered in order to suppress the total energy

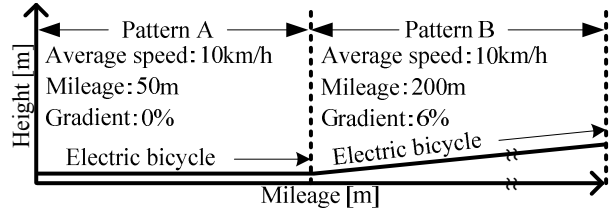


Fig. 2. Assist pattern of driving test.
The assist assume only two patterns.

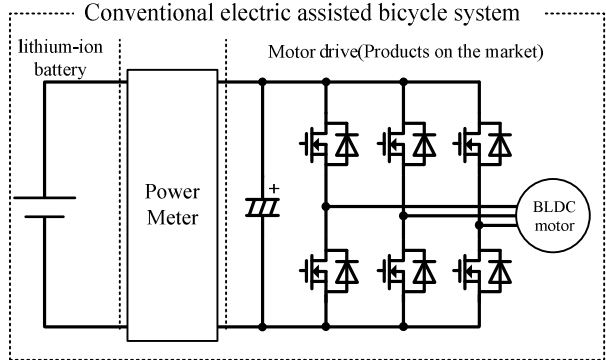
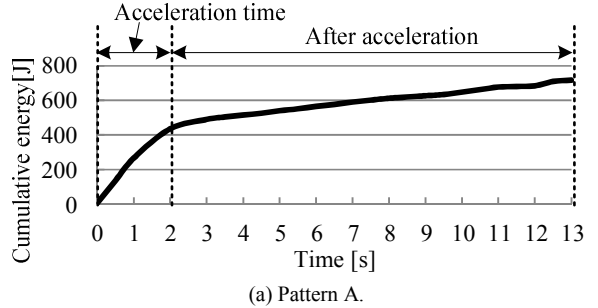
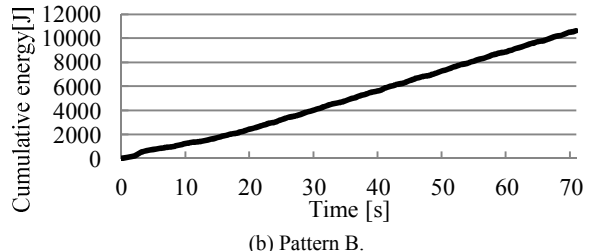


Fig. 3. Method of measuring the cumulative energy of each assist pattern.



(a) Pattern A.



(b) Pattern B.

Fig. 4. Time characteristics of the cumulative energy of each assist pattern. The cumulative energy is measured based on the conditions of Figure 2.

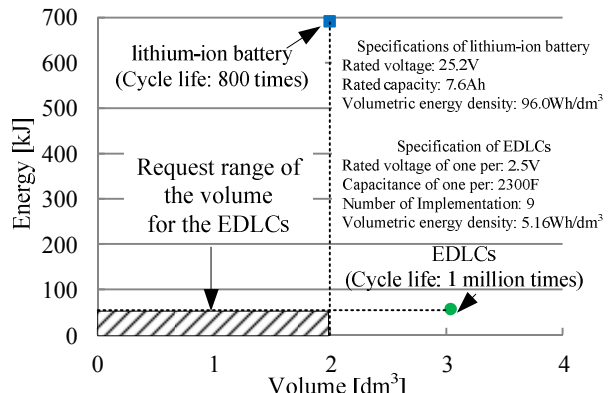


Fig. 5. Relationship between energy and volume of EDLCs and lithium-ion battery.

The request range of volume for EDLCs is shown.

capacity, the proposed system becomes useful. Therefore, operation verification of the system is discussed as a 200m distance in Chapter 6.

IV. DESIGN OF ANTENNA FOR WIRELESS POWER TRANSMISSION AND CHARGER

A small receiving antenna is preferred in order mounting to the electric bicycle. Therefore, the authors have been proposed a formula spiral antenna made of a printed circuit board, which is flat, compact and easy design.

A. Design of Wireless Charger

Fig. 6 shows the structure and equivalent circuits of the transmitting antenna for wireless power transmission. The connection point of the short type and open type is the output of a RF power supply. For the receiving antenna, the equivalent circuit is the same. The antenna has a two-layer structured wiring in order to increase the inductance value.

Fig. 7 shows the design flow chart of the charger and the antenna for the wireless power transmission. From Fig. 7, the charging power is determined by the charging time and the charging energy. The antenna is designed from the specifications of the antenna size and the charging power. The charger considers the short charging time and the volume of power conversion system for the charging power. The target of charging time T is 60 sec, and the charging energy E is supplied to 56.5 kJ. In addition, the average output power of the charger E/T is 1 kW. However, the size of the circuit becomes large when the charging circuit combines with the discharging circuit. Therefore, the charging control should be placed in RF power supply of the power transmission side of the wireless power transfer system is realistic.

Also, the antenna size depends on the mounting position of the power receiving side. The antenna for wireless power transmission is experimentally compared the short type and open type with the same size.

B. Comparison of Transmission Efficiency

Fig. 8 shows the system configuration of the experiments. Arbitrary frequency is output using a function generator. The output power cannot output 1 kW(The average output power of the charger) because of capacity limit of RF power supply. Therefore, the output of the RF power supply is scaled to 100W (10% of 1kW). Reflected power P_R is measured using a power meter in the front stage of the power transmission antenna. Also, the antenna of short type is connected in series with the capacitor of capacitance 500 pF.

Fig. 9 shows the experimental results of the frequency characteristics of the transmission efficiency. The power is amplified by the amplifier. The antenna is designed according to the flowchart of Fig. 7. From Fig. 9, it is confirmed that the short type can realize the low resonance frequency compared to the open type at the same transmission efficiency and antenna size. In general,

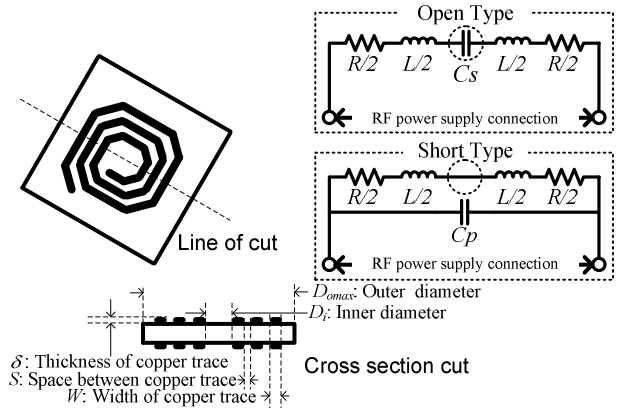


Fig. 6. Structure of the antenna for wireless power transmission. The antenna is a printed circuit board of the two layers.

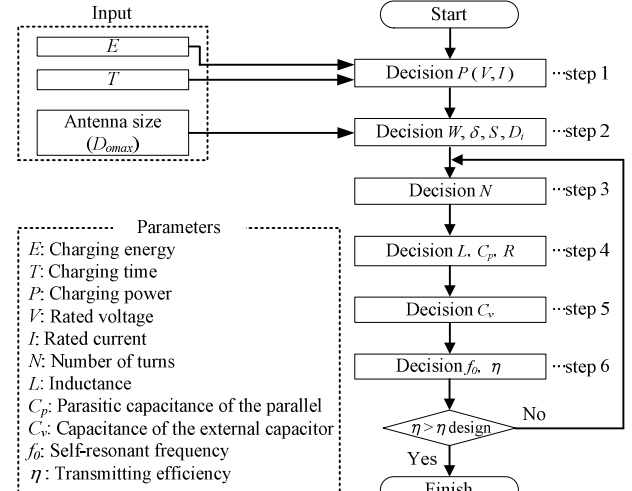


Fig. 7. Design flow chart of charger and antenna for wireless power transmission. Specifications of the antenna is determined by the antenna size and the charging power.

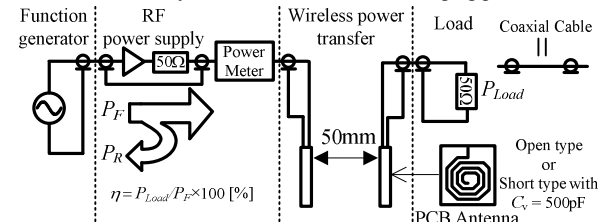


Fig. 8. System configuration of the experiments. The system of the experiment circuit is matched at 50Ω .

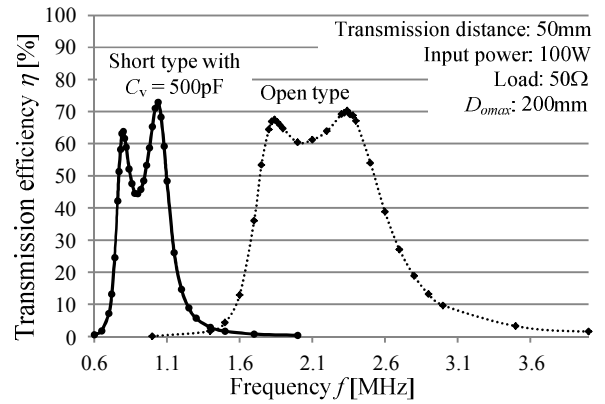


Fig. 9. Experimental results of the frequency characteristics of the transmission efficiency.

It is the result of the experiment under the same conditions.

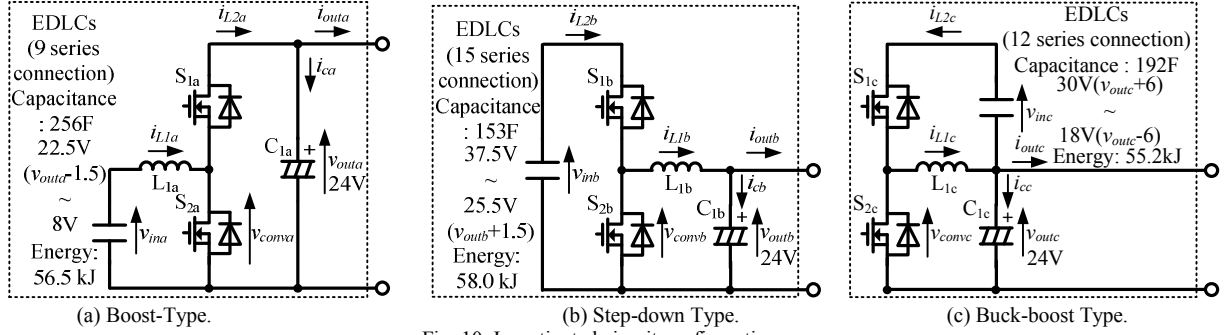


Fig. 10. Investigated circuit configuration.

The EDLCs of a circuit of three types are designed with the same energy.

If resonant frequency (Frequency of RF power supply) is the low frequency, the efficiency of RF power supply is high. Therefore, the short type can be high efficiency of the system than the open type. So, the proposed system is adopted the short type.

V. DESIGN OF THE INTERFACE CONVERTER FOR EDLCs

A. Circuit configuration to be compared

Fig. 10 shows the circuit configuration of three kinds of DC-DC converters. This paper investigates the step-down type, boost-type and buck-boost type as the charging and discharging DC-DC converter by using EDLCs. The number and the output voltage range of the EDLCs are designed when the charging and discharging energy of EDLCs meet more than 53.0 kJ. Thus, the DC-DC converters are designed that the charging and discharging energy of EDLCs is as follows: the energy of the boost-type, step-down type and buck-boost type are 56.5 kJ, 58.0 kJ and 55.2 kJ, respectively. In addition, the specification of the input voltage of the DC-AC converter is 24 V (V_{outa} , V_{outb} , V_{outc}), and the output voltage of the DC-DC converter is controlled to 24 V at constant. Further, the reactors of all types are designed to the current ripple value (1.5 A) as same as the step-down type. Therefore, the reactors of all types are designed that the current ripple of the reactor meets less than 1.5A. On the other hand, the smoothing capacitor is designed from the allowable ripple current.

In this system, by the force step on the pedal of a bicycle, the energy, which is used for an assist, and the load of BLDC motor are changed. It is necessary to increase the capacitance of the smoothing capacitor in order to reduce the variation in the output voltage of the DC-DC converter owing to load variations. However, the volume of the smoothing capacitor should be reduced in terms of volume implementation. Therefore, when the load fluctuations occur, it is important to reduce the volume of the smoothing capacitor by implementing the fast control response of the output voltage [11].

B. Comparison of Power Loss

Fig. 11 shows the power loss analysis of three kinds of DC-DC converters when the voltage of the EDLCs V_{in} is changed. The power loss is analyzed under the conditions that the output power of the DC-DC converter is 384 W.

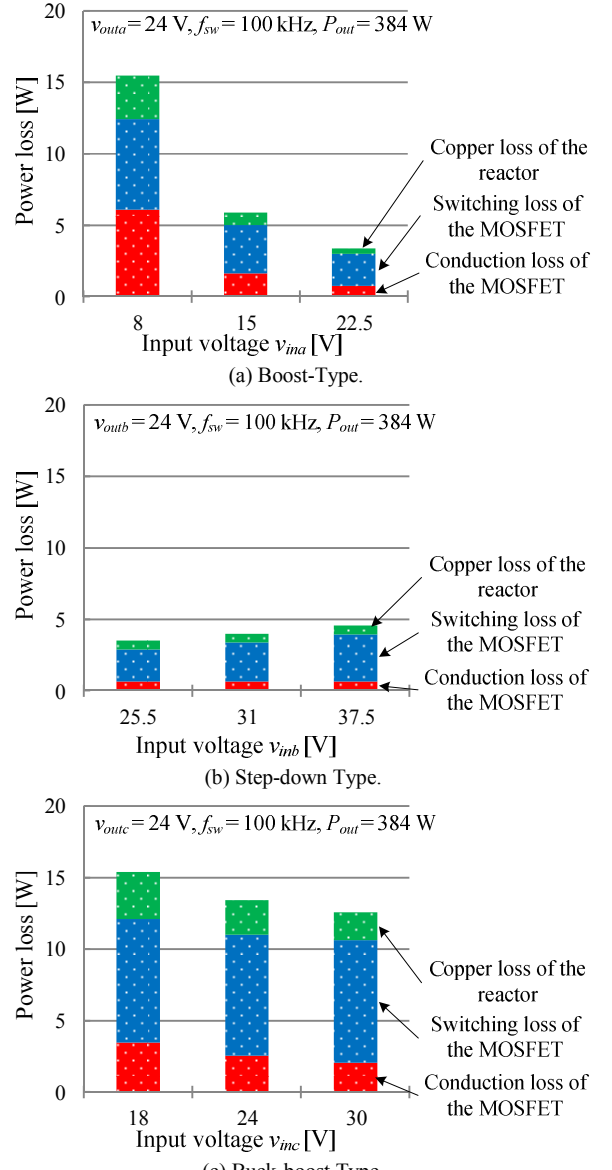


Fig. 11. Results of power loss analysis of the three kinds of DC-DC converters.

The power loss is neglected iron loss of the reactor, the conduction loss of the diode, recovery loss.

It is noted that dead time is neglected. As shown in Fig. 11, it is confirmed that the switching loss and the conduction loss of the MOSFET dominates the total loss

in the boost-type. Also, it is confirmed that the switching loss of the MOSFET is dominates the total losses in the step-down type and buck-boost type. This is because the input current of the boost-type is increased owing to the input voltage, which is lower than the step-down type and buck-boost type.

C. Comparison of Total Volume

Fig. 12 shows the relationship between the total volume and the output power for the three kinds of DC-DC converters. It is noted that the power loss is maximum for the voltage of EDLCs in Fig. 11. In addition, the volume of the Fig. 12 is the sum of volume of EDLCs and DC-DC converter (Reactor, Heat sink, Electrolytic capacitor).

In this paper, CSPI (Cooling System Performance Index), which is a reciprocal of the product of the volume and the thermal resistance, is introduced to estimate the volume of cooling system. The CSPI indicates the cooling performance per unit volume of the cooling system. It means that a high performance cooling system shows high CSPI. Therefore, the cooling system is miniaturized when CSPI become higher. The volume of the cooling system $vol_{cooling}$ is given by (2) from the relationship between the power loss and the rise in temperature [12].

$$vol_{cooling} = \frac{1}{R_{th} \times CSPI} = \frac{P_{loss}}{(T_j - T_a) \times CSPI} \quad (2)$$

where R_{th} is the thermal resistance of the cooling system, T_j is the junction temperature of the switching device, T_a is the ambient temperature, P_{loss} is the power loss of the switching device.

In this paper, the reactor is designed by the Area Product concept [13] using a window area and a cross-sectional area. Then volume of the reactor vol_L is given by (3).

$$vol_L = K_v \left(\frac{2W}{K_u B_m J} \right)^{\frac{3}{4}} \quad (3)$$

where K_v is the constant value depending on the shape of cores, W is the maximum energy of the reactor, K_u is the occupancy of the window, B_m is the maximum flux density of the core, and J is the current density of the wire.

The capacitor volume is calculated based on commercially available electrolytic capacitors [14]. The volume of the electrolytic capacitor is proportional to the rms value of the ripple current of the electrolytic capacitor. The volume vol_{CE} of the electrolytic capacitor is given by (4).

$$vol_{CE} = \gamma_{VCE}^{-1} I_{CRMS} \quad (4)$$

where γ_{VCE} is the proportionality factor between the rms value of the ripple current and the volume, and I_{CRMS} is the rms value of the ripple current of the electrolytic capacitor.

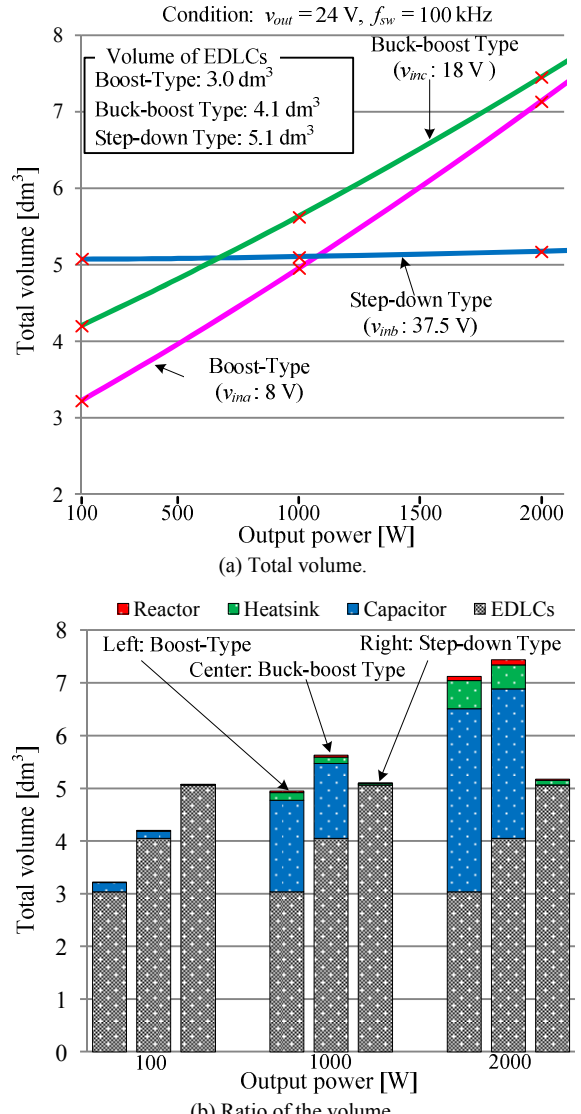


Fig. 12. Relationship between the total volume and the output power for the three kinds of DC-DC converters.

From Fig. 12 (b), around the output power of 100 W, the volume of the EDLCs is dominant in the converter of all types. The number of EDLCs for the boost-type is the fewest in all of other DC-DC converters. Therefore, the volume of the boost-type is the smallest. However, if the output power is 1.1 kW or more than 675 W, the volume of the step-down type is smaller than that of the boost-type and the buck-boost type. For the boost-type and the buck-boost type, the ripple current of the smoothing capacitor is increased when the output power is increased. Therefore, the ratio of the volume of the smoothing capacitor is increased. On the other hand, for the step-down type, the ripple current of the smoothing capacitor does not depend on the output power. Therefore, when the output power is increased, therefore, when the output power is increased, the volume of heat sink and reactor which is very small compared to the volume of the EDLCs is increased. However, the volume of the converter does not increase too much. Furthermore, if the output voltage of the DC-DC converter is set to over 24V, the cross over point of the volume of three kinds of DC-

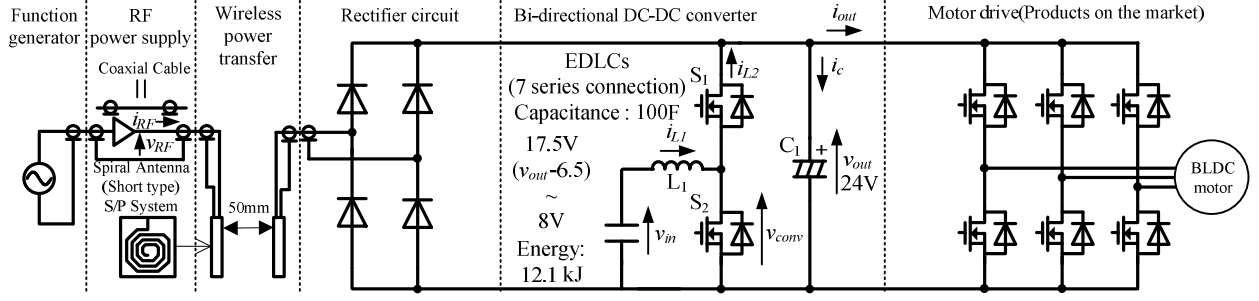


Fig. 13. The entire circuit diagram of the proposed system.
The proposed system is designed based on the system design to chapter 5.

DC converter is shifted toward high output power. The reason is that the volume of the capacitor is decreased depends on its ripple current according to the high output voltage of the DC-DC converter. Also, boost-type is the most compact in the power capacity (384W) of the electric assisted bicycle. So, the proposed system is adopted the boost-type.

VI. CHARGING VERIFICATION OF SYSTEM

A. Design of the whole system

Fig. 13 shows the circuit diagram of the entire system based on the system design to chapter 5. By the system design, the total volume of boost type is most minimum in three kinds of DC-DC converters at the maximum power (384W) of electric assisted bicycle. Therefore, boost type is adopted for the bi-directional DC-DC converter. In the antenna for wireless power transmission, the short type can be high efficiency of the RF power supply than the open type. Therefore, the antenna of short type is adopted. The running distance of a slope is more than 200 m as prototype specifications in this paper. Thus, the energy of the EDLCs (Nippon Chemi-Con Co, DDLE2R5LGN701KAA5S) is designed in 12.1 kJ [10]. In addition, the specification of the charging time is 1 minute. The wireless power transfer system is adopted the S/P system [15].

Fig. 14 shows the equivalent circuit diagram of the S/P system. The transmitting antenna is connected to the RF power supply. The receiving antenna is connected to the rectifier.

Table I shows the specification of antenna for wireless power transmission. The designed coupling factor and the self-inductance are measured by a LCR meter. The capacity C_2 of the parallel capacitor is given by (5). The capacity C_1 of the series capacitor is given by (6).

$$C_2 = \frac{1}{L_2 \omega_0^2} \quad (5)$$

$$C_1 = \frac{1}{(1 - k_0^2)L_1 \omega_0^2} \quad (6)$$

where L_2 is the self-inductance of receiving antenna, ω_0 is the resonance angular frequency, k_0 is the designed coupling factor, L_1 is the self-inductance of transmitting antenna.

Fig. 15 shows the control block diagram of wireless charging. In the S/P system, If the voltage of transmitting

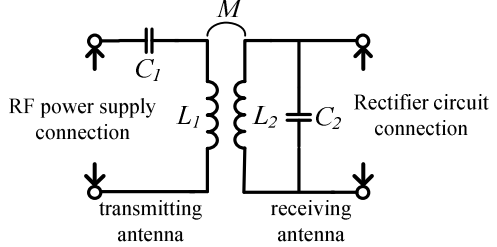


Fig. 14. Equivalent circuit diagram of the S/P system.
The capacitor is connected to an external antenna.

Table I. Specification of antenna.

Items	Values	Remarks
Outline (Length)	250 mm	
Outline (Side)	200 mm	
Number of turns (surface)	10 turn	Short type
Number of turns (reverse face)	10 turn	Short type
Space between copper trace	5 mm	
Width of copper trace	3 mm	
Thickness of PCB	2 mm	FR-4
Thickness of copper trace	70 μm	
Self-inductance L_1	58.27 μH	
Self-inductance L_2	58.70 μH	
Mutual inductance M	21.95 μH	
Designed coupling factor k_0	0.375	
Primary capacitance C_1	586 pF	
Secondary capacitance C_2	500 pF	

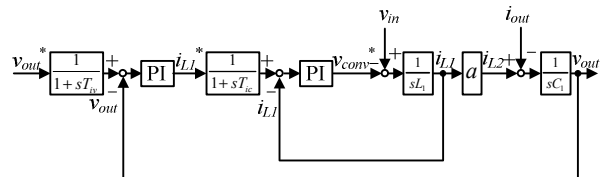


Fig. 15. Control block diagram.
The output voltage of bi-directional DC-DC converter is controlled to a constant 24V.

Table II. Conditions of the experiment.

Items	Values	Remarks
Frequency of the FG	929 kHz	
Resonant frequency	929 kHz	
Voltage of the FG	450 mVrms	
Gain of the RF power source	100	
Transmission distance	50 mm	

antenna is not controlled, the voltage of the power receiving antenna is varied by variation of the coupling coefficient and load [16]. In this problem, the breakdown voltage of the switching elements must be designed by taking into account the variation of the coupling coefficient and the load. Therefore, charging control by the combination of two points as below is proposed.

1) The output voltage of the bi-directional DC-DC converter is controlled to be constant.

2) The output voltage of the RF power supply is set higher than the output voltage of the bi-directional DC-DC converter.

Thus, the design of the breakdown voltage of the switching device can be simplified. The charging experiment is based on the experimental conditions shown in Table II.

B. Experimental results of charging

Fig. 16 shows the experimental results of the wireless charging to the EDLCs.

Fig. 16(a) shows the voltage and current waveform of the input and output for the bi-directional DC-DC converter. From Fig. 16 (a), the output voltage of the bi-directional DC-DC converter is controlled to be constant, and the EDLCs are charged.

Fig. 16(b) shows the energy storage capacity of EDLCs from the start of charging to the end of charging. From Fig. 16 (b), the energy capacity of the EDLCs are charged from 0% to 100% in about 6 minutes is confirmed. The reason that charging time is not within 1 minute is for the capacity limit of the RF power supply used in experiments of this paper. Therefore, the charging can be achieved a full charging in 1 minute using the high-capacity RF power supply.

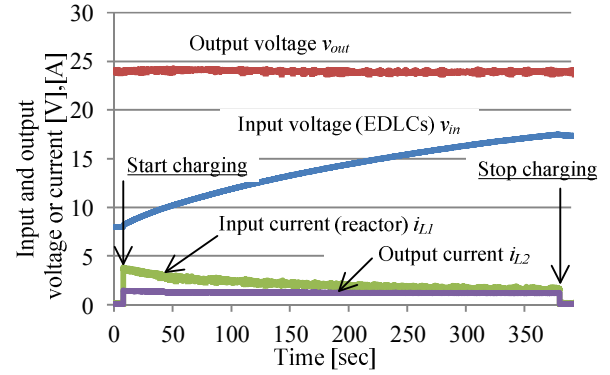
Fig. 16(c) shows the output voltage and current waveforms of the RF power source, input voltage waveform of bi-directional DC-DC converter, voltage waveform of EDLC (The voltage of EDLC is at the 8V). From Fig. 16 (c), the input power factor of the high frequency power source is approximately 1 is confirmed.

Fig. 17 shows the comparison of the charging time for charging the 12.1kJ of the proposed system and conventional system. The charging energy of the conventional system is calculated from specification of the product. From Fig. 17, the proposed system can shorten to 1/4 the charging time of the conventional system.

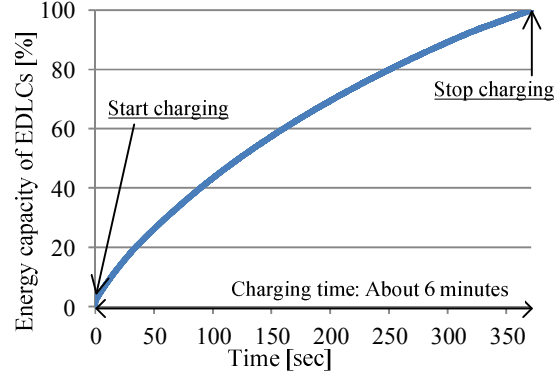
C. Wireless charging method

Fig. 18 shows the wireless charging method to the electric assisted bicycle. The receiving antenna is connected to the sides of the front basket of the electric assisted bicycle. The proposed system is introduced to a charging side. There are the following advantages by this method.

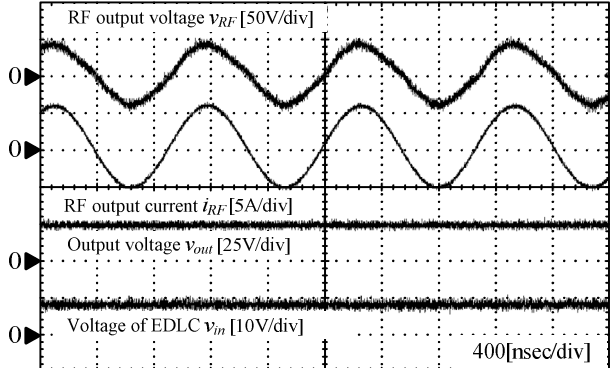
1) The foreign body (Dust, etc) is less likely to adhere to the power transmitting and receiving antenna, as compared to a system for power transmission from the ground (Therefore, it does not affect the transmission



(a) voltage and current waveform of the input and output.



(b) Energy capacity of EDLCs.



(c) Waveform(Voltage of EDLCs is at the 8V).

Fig. 16. Experimental results of the wireless charging to the EDLCs

The energy capacity of EDLCs is the wireless charging in about 6 minutes.

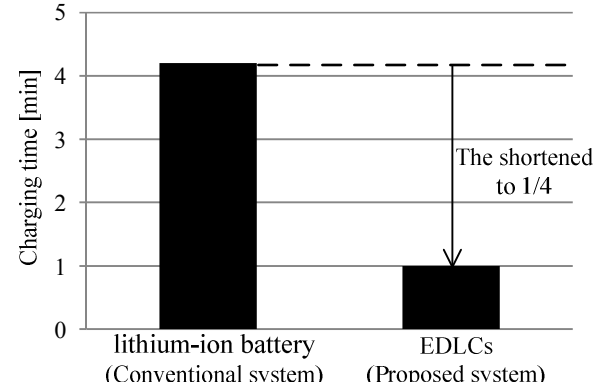


Fig. 17. Comparison of the charging time for charging the 12.1kJ of the proposed system and conventional system.

The proposed system can be charged rapidly than conventional system.

efficiency)

2) The variation of transmission distance and the positional deviation of between the transmitting and receiving antenna can be reduced by the front wheel is fixed using bicycle parking stand.

3) It is low cost because the antenna and wiring are not placed into the ground.

VII. CONCLUSION

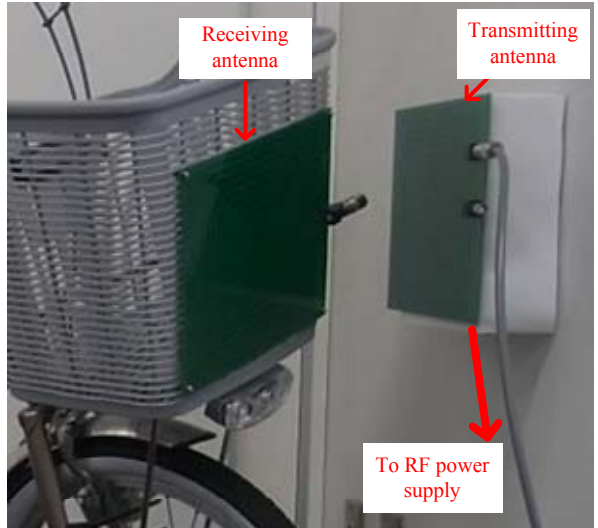
This paper evaluated the energy capacity of EDLCs, the antenna for wireless power transmission and the charger, the interface converter for EDLCs in proposed system configuration. The proposed system was experimentally verified as prototype.

The results showed that the short type as the antenna for wireless power transmission can be to system of higher efficiency than the open type with the same size. Also, the results showed that the total volume of the boost-type DC-DC converter is the smallest when the output power is less than 1.1 kW. Therefore, in terms of the volume of the system at the minimum point, the boost-type DC-DC converter is suitable for the electric assist bicycle. Also, the results showed that the proposed system can shorten to 1/4 the charging time of the conventional system.

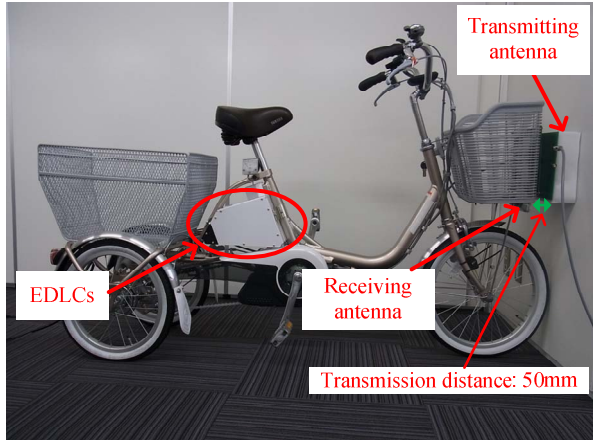
In the future work, the proposed system will be experimentally verified running test in an actual road.

REFERENCES

- [1] Y. Hori: "Future vehicle society based on electric motor, capacitor and wireless power supply", *IEEE IPEC2010*, pp.2930 – 2934 (2010)
- [2] A. Govindaraj, M. King, S. M. Lukic: "Performance characterization and optimization of various circuit topologies to combine batteries and ultra-capacitors", *IEEE IECON2010*, pp 1850-1857 (2010)
- [3] K. Noguchi, K.Orikawa, J. Itoh: "System Design of Electric Assisted Bicycle using the EDLCs as Power Source", *2013 Japan-Korea Joint Technical Workshop on Semiconductor Power Conversion*, No. IEEJ-SPC-P2-21 (2013) (in Japanese).
- [4] A. Kurs, A. Karalis, R. Moffatt, J. D. Joannopoulos, P. Fisher, M. Soljacic: "Wireless Power Transfer via Strongly Coupled Magnetic Resonances", *Science*, Vol. 317, pp. 83-86 (2007)
- [5] S. Lee, R. D. Lorenz: "Development and Validation of Model for 95%-Efficiency 200-W Wireless Power Transfer Over a 30-cm Air-gap", *IEEE Trans. On Industry Applications*, Vol. 47, No. 6, pp. 2495-2504 (2011)
- [6] C.S. Wang, O.H. Stielau, and G.A. Covic. "Design Considerations for a Contactless Electric Vehicle Battery Charger", *IEEE Trans. On Industrial Electronics*, Vol. 52, No. 5, pp. 1308-1314 (2005)
- [7] T. Imura, Y. Hori: "Maximizing Air Gap and Efficiency of Magnetic Resonant Coupling for Wireless Power Transfer Using Equivalent Circuit and Neumann Formula", *IEEE Trans. On Industrial Electronics*, Vol. 58, No. 10, pp. 4746-4752 (2011)
- [8] A. P. Sample, D. A. Meyer, J. R. Smith: "Analysis, Experimental results, and Range Adaptation of Magnetically Coupled Resonators for Wireless Power Transfer", *IEEE Trans. On Industrial Electronics*, Vol. 58, No. 2, pp. 544-554 (2011)
- [9] Yamaha Motor Co., Ltd. PAS wagon.
(<http://www.yamaha-motor.jp/pas/lineup/wagon/>)
- [10] Nippon Chemi-Con Co.
(<http://www.chemi-con.co.jp/catalog/dl.html>)
- [11] T. Shibuya, J. Itoh: "An Evaluation of optimal Design of Capacitance by High Speed of a Control Response", *SPC Osaka*, No. SPC-12-026 (2012) (in Japanese).
- [12] U. DROFENIK, G. LAIMER, and J. W. KOLAR: "Theoretical Converter Power Density Limits for Forced Convection Cooling" *International PCIM Europe Conference*, pp.608-619 (2005)



(a) Attached photo of the antenna.



(b) The entire photo.

Fig. 18. Wireless charging method to the electric assisted bicycle.

- [13] Wm. T. Mclyman: "Transformer and inductor design handbook", Marcel Dekker Inc. (2004)
- [14] Y. Kashihara, J. Itoh: "Parfomance Evaluation among Four types of Five-level Topologies using Pareto Front Curves", *IEEE ECCE 2013*, pp.1296-1303 (2013)
- [15] S. Lee, R. D. Lorenz: "A Design Methodology for Multi-kW, Large Airgap, MHz Frequency, Wireless Power Transfer Systems", *IEEE ECCE 2011*, pp. 3503-3510 (2011)
- [16] K. Takuzaki, N. Hoshi: "Consideration of Operating Condition of Secondary-side Converter of Inductive Power Transfer System for Obtaining High Resonant Circuit Efficiency", *IEEJ Trans. IA*, Vol. 132, No. 10, pp. 966-975 (2012) (in Japanese).